Optical Probing of Laser-Produced Plasma Experiments on the OMEGA EP Laser System

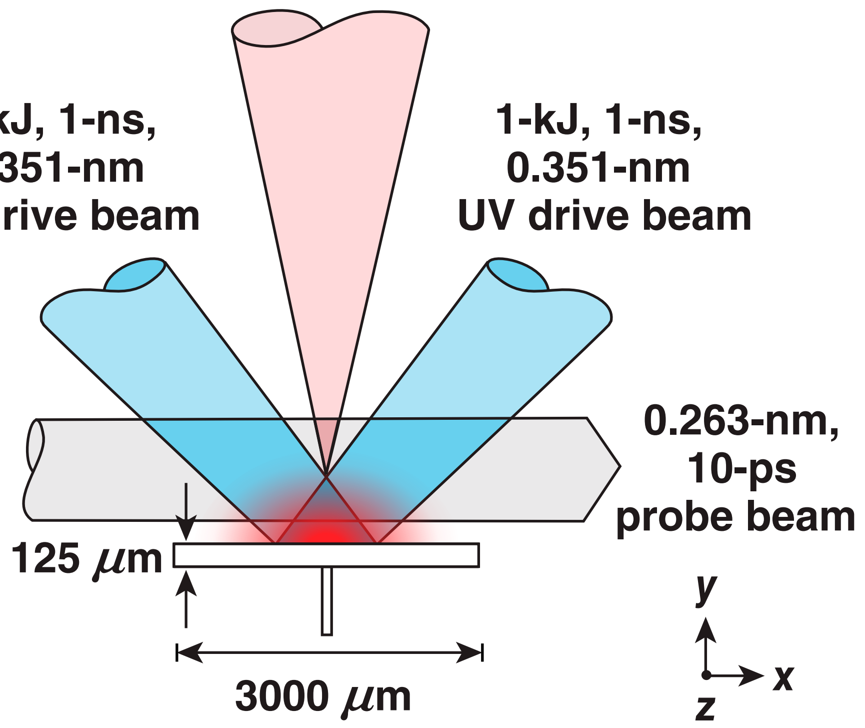

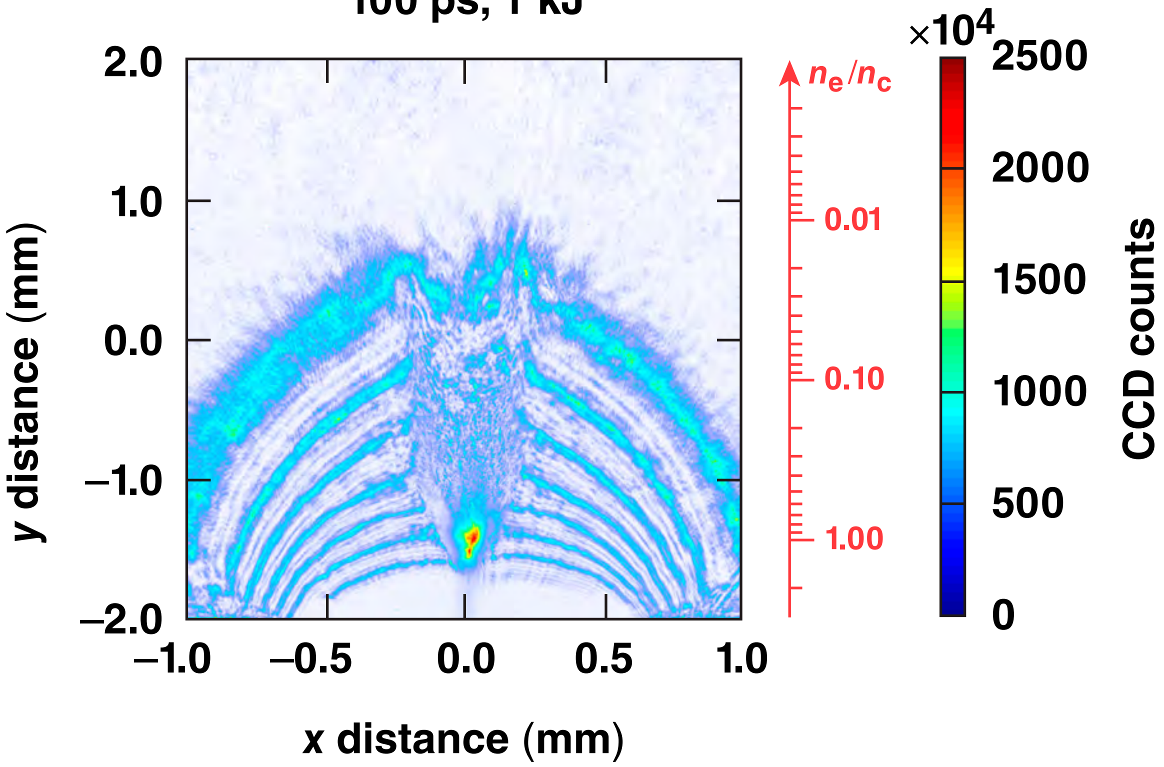

S. Ivancic
University of Rochester
Laboratory for Laser Energetics

45th Annual Anomalous Absorption Conference
Ventura, CA
14–19 June 2015

Summary

OMEGA EP experiments show for the first time the guiding of a high-intensity pulse to beyond critical density in a fast-ignition (FI)–relevant, long-scale-length plasma

- Angular filter refractometry (AFR)* is used to observe the density modification of a channel beyond critical IR density (1.4×10^{21} cm^{-3})
- A high-intensity (>10^{18} W/cm^2) laser evacuates a conical-shaped cavity with ~65% lower density than the background density
- A 100-ps, 1-kJ laser pulse produced a channel beyond critical, allowing for the efficient transmission of a high-intensity ($I \cong 4 \times 10^{19}$ W/cm^2) co-propagated pulse to beyond critical density

*D. Haberberger *et al*., Phys. Plasmas 21, 056304 (2014).

Collaborators

D. Haberberger, C. Stoeckl, K. S. Anderson, C. Ren, W. Theobald,
J. Fienup, D. H. Froula, and D. D. Meyerhofer

University of Rochester
Laboratory for Laser Energetics

T. Iwawaki, H. Habara, and K. Tanaka

Osaka University

Fast ignition* relies on the isochoric heating of compressed thermonuclear fuel assemblies

- Thermonuclear fuel is compressed via spherical rocket drive to high density
- Electrons,* protons,** and soft x rays*** can be used but assembled fuel must have sufficient stopping power
- The ponderomotive potential of intense laser pulses (>10^{18} W/cm^2) creates a beam of electrons in the MeV range

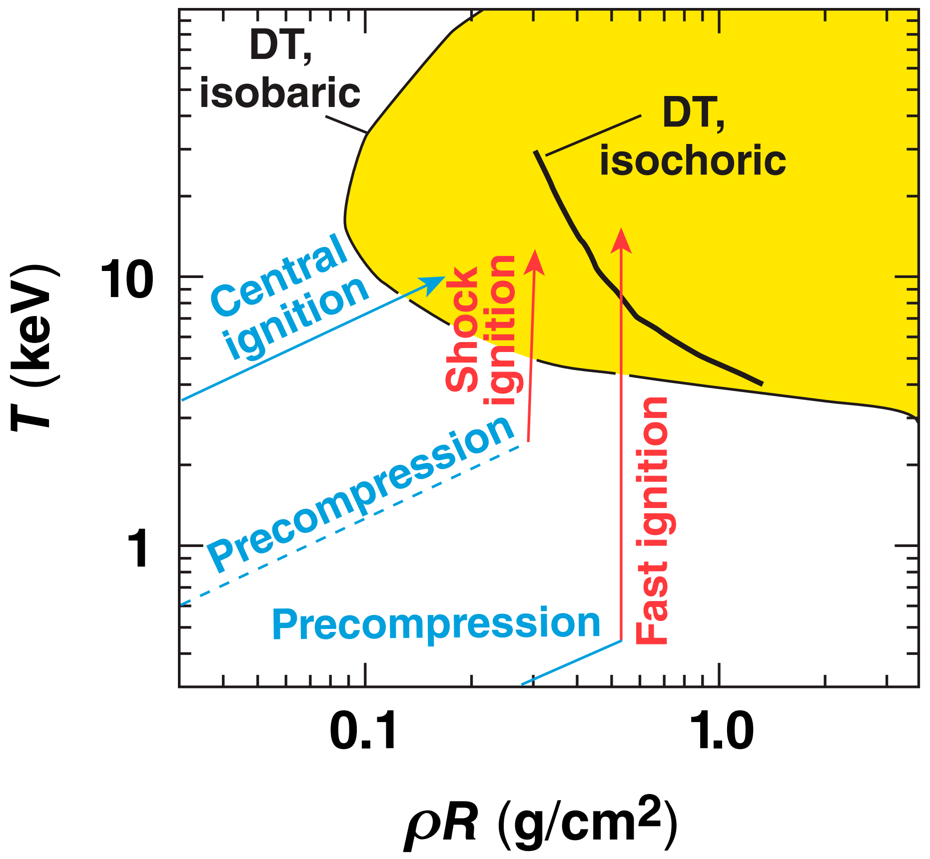

For electron FI, the goal is to get the source close to the compressed core.

*M. Tabak *et al*., Phys. Plasmas 1, 1626 (1994).
**M. Roth *et al*., Phys. Rev. Lett. 86, 436 (2001).
***S. X. Hu, V. N. Goncharov, and S. Skupsky, Phys. Plasmas 19, 072703 (2012).

E23523a

Cone-in-shell experiments* have provided one method to deliver an electron beam to the core

- Cone-tip breaks out ~200 ps ahead of peak compression
- Integrated *DRACO–LSP* simulations show that most of the electron beam is lost in the gold cone

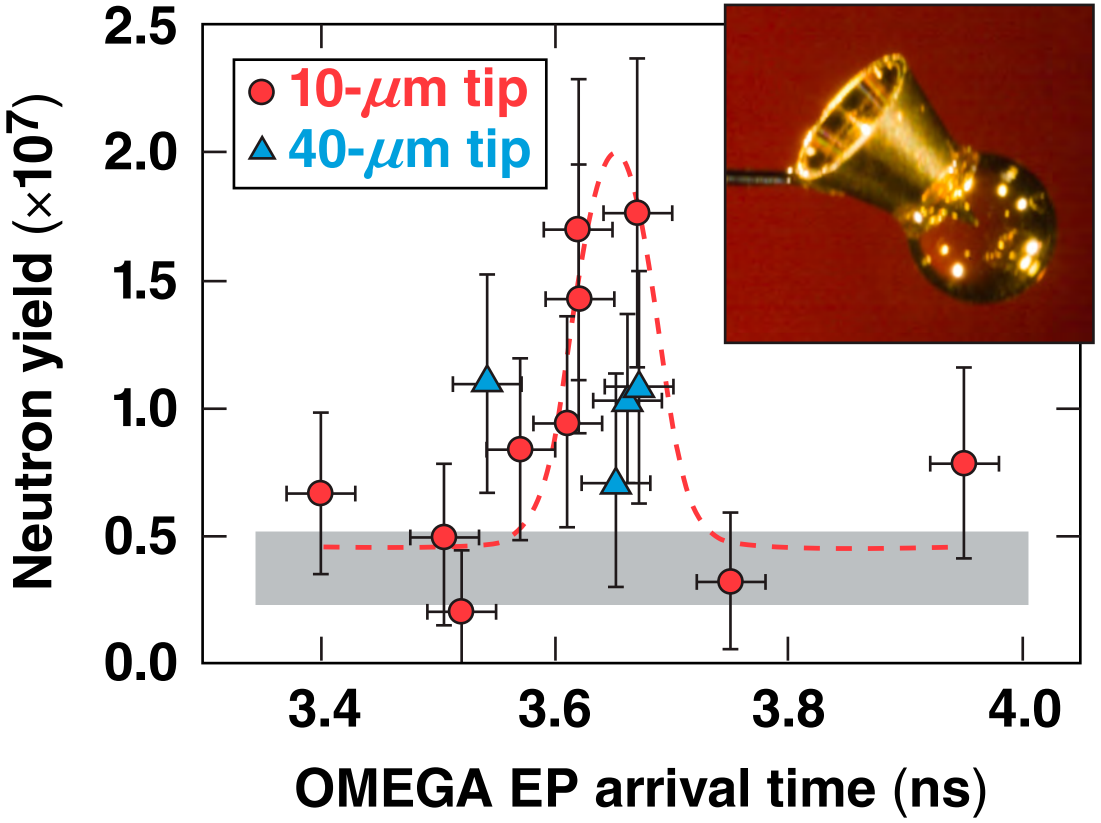

10-ps, 1-kJ short pulses**

Electron transport through the cone may inhibit heating of the core.

*R. Kodama *et al*., Nature 412, 798 (2001).
**W. Theobald *et al*., Phys. Plasmas 18, 056305 (2011).

Channeling through the corona of an imploded capsule offers an alternative to cone-in-shell targets

Fast heating with ultra-intense laser beams*

Measurements

- Forward-going velocity of the channel in a FI-relevant plasma
- Density depletion inside the channel
- Duration of channel existence

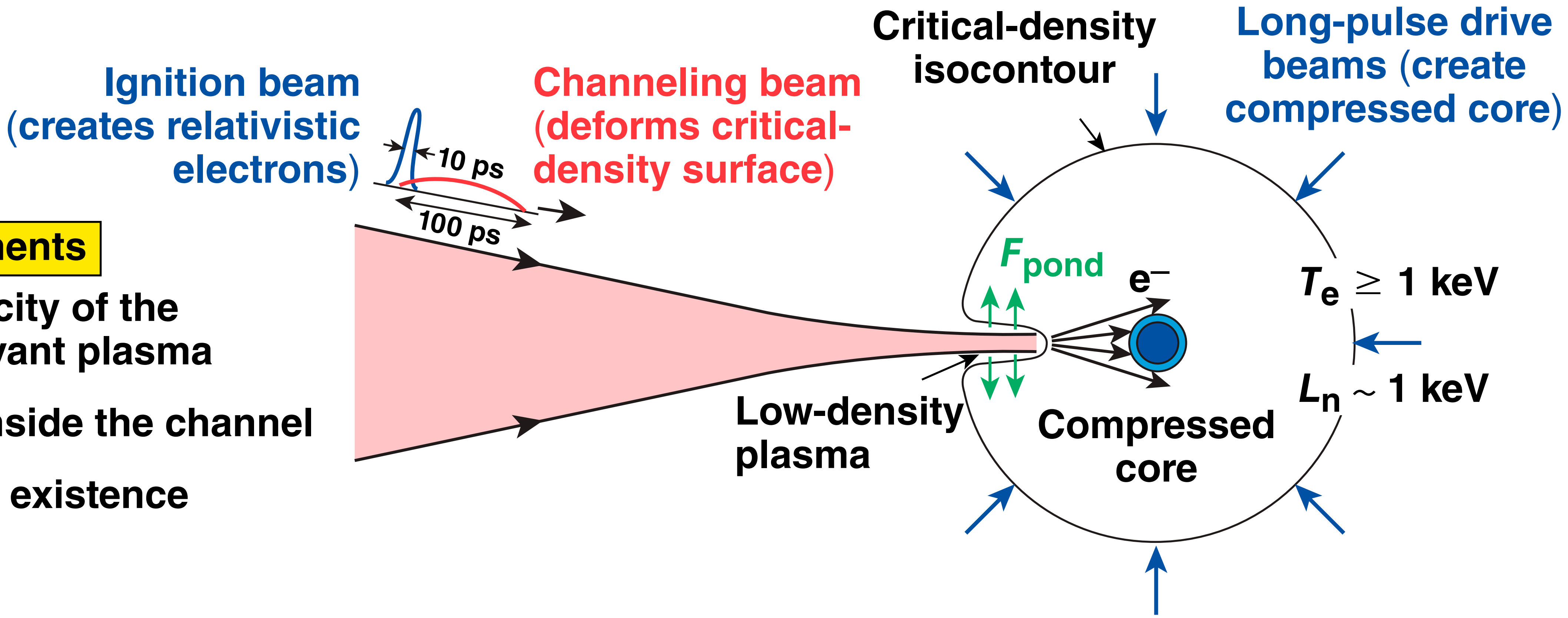

E23540a

*M. Tabak *et al.*, Phys. Plasmas 1, 1626 (1994).

Channeling experiments were performed using five high-power laser beams on OMEGA EP

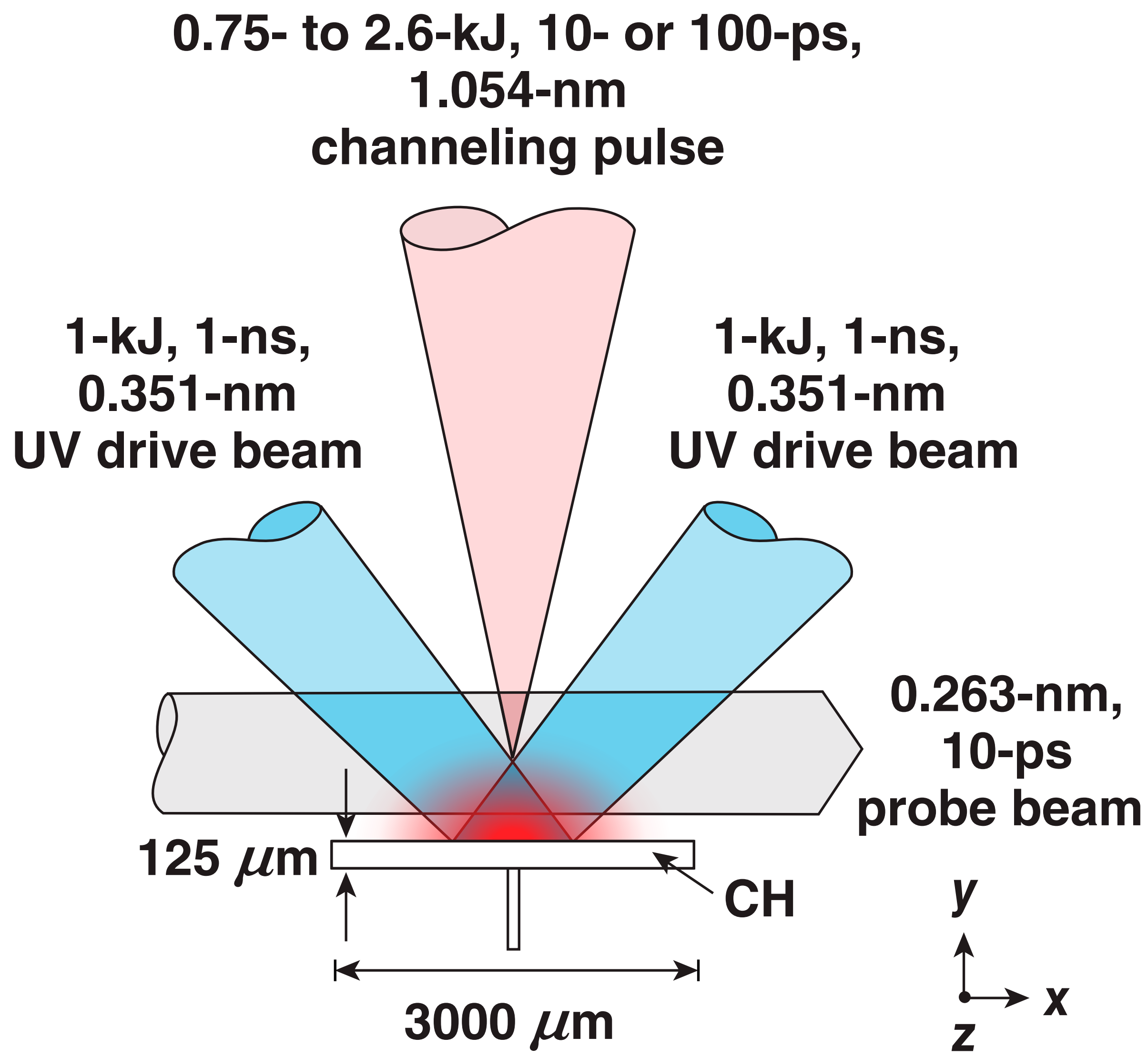

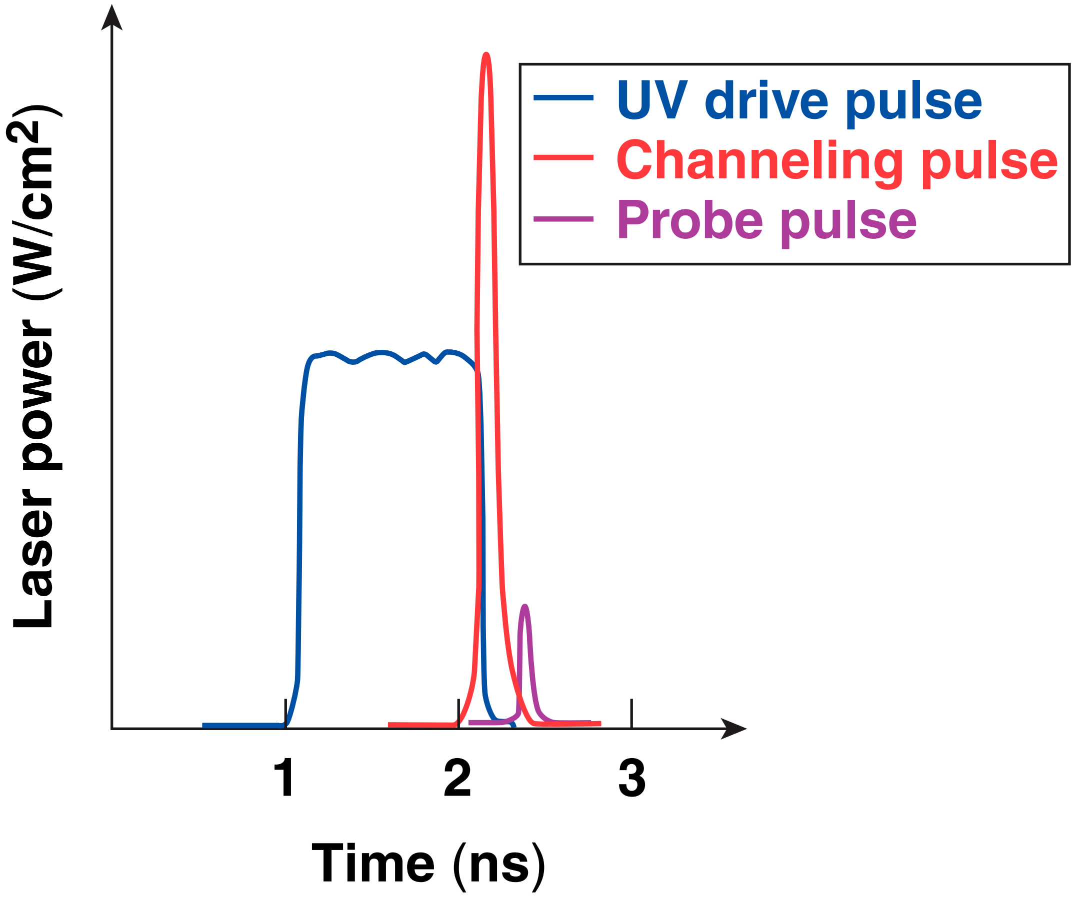

E23460

AFR filters rays as a function of refracted angle only

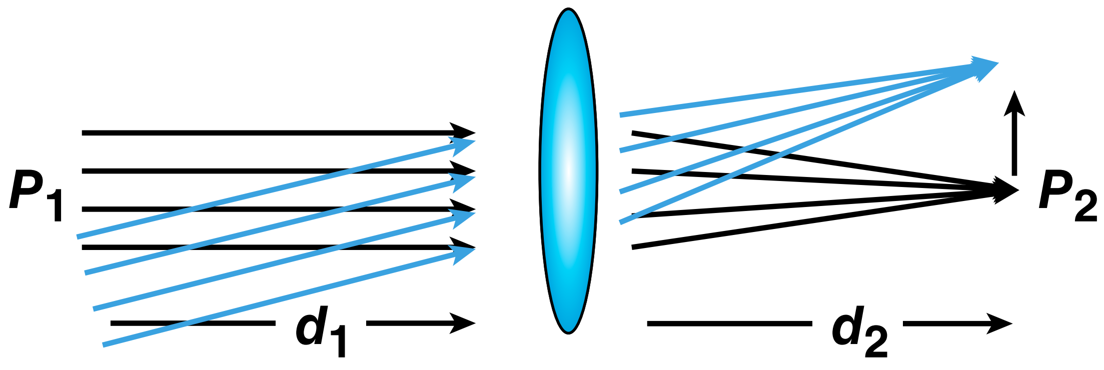

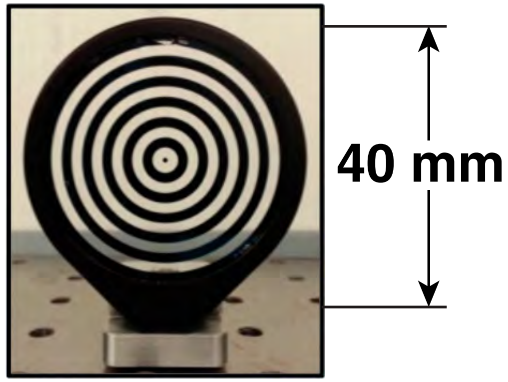

AFR filter

$$\frac{1}{d_1} + \frac{1}{d_2} = \frac{1}{f_{eff}}$$

- The ray-transfer matrix between our probing plane P_1 and the filter plane P_2 is given by

$$\begin{pmatrix} y_2 \\ \theta_2 \end{pmatrix} = \left[\begin{pmatrix} 0 & \frac{f_{eff}}{n_1} \\ \frac{n_1}{f_{eff}} & 0 \end{pmatrix}\right] \begin{pmatrix} y_1 \\ \theta_1 \end{pmatrix}$$

At the filter plane the position of the ray y_2 is determined solely by the input angle θ_1.

E24216

The relation between radial position on the filter and the refraction angle is determined *in-situ*

AFR calibration image with a f = –20-mm lens

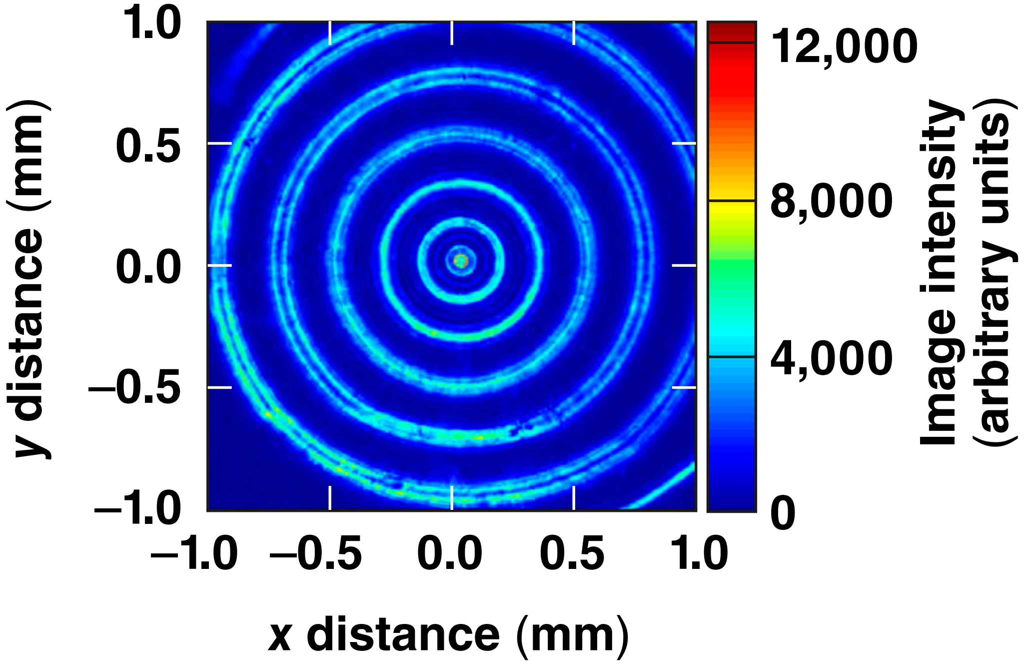

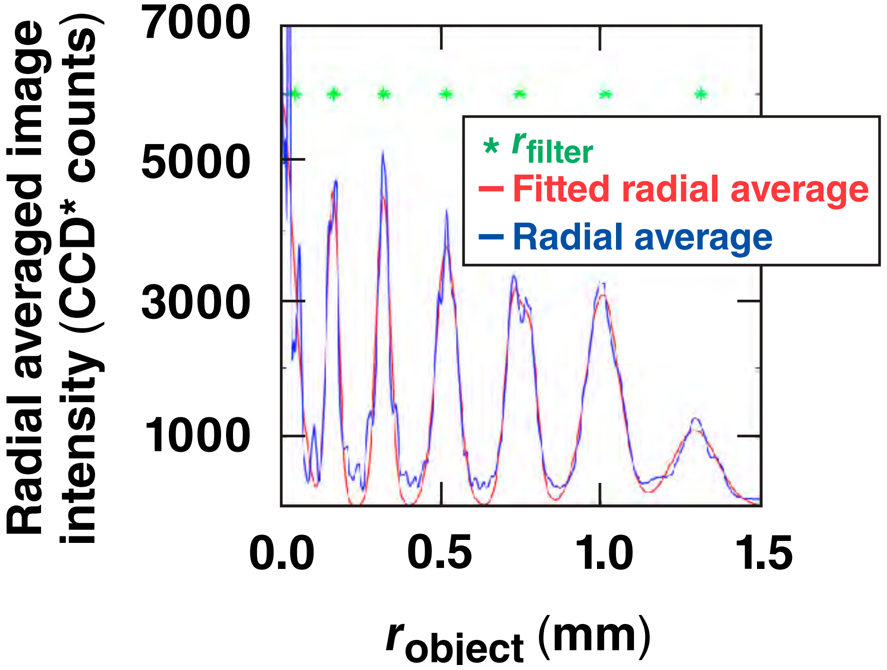

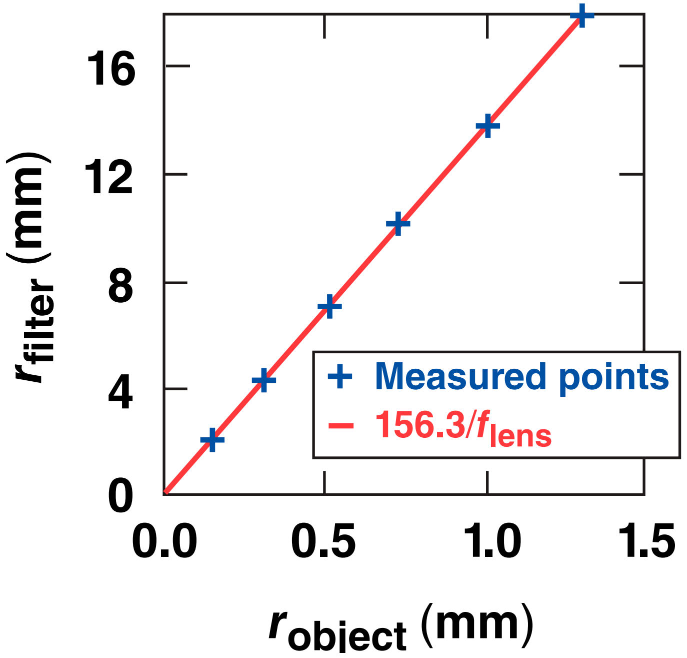

$$\theta^\circ = (0.365 \pm 0.003) \times r \text{ (mm)}$$

The angular filter calibration is linear over the range of angles probed.

*CCD: charge-coupled device

The experimental AFR images are analyzed using the calibration angles

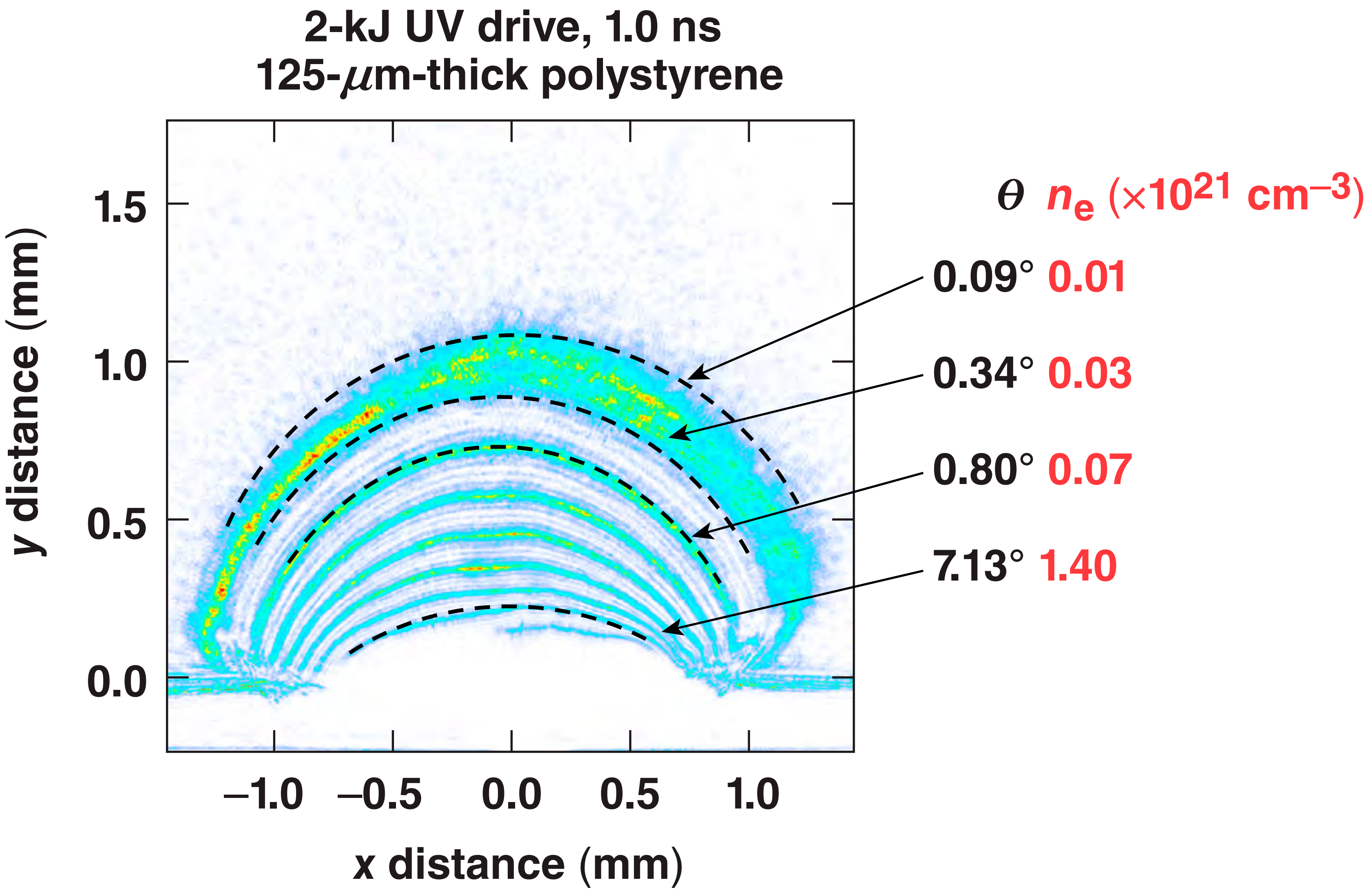

E24220

Agreement between radiation–hydrodynamics simulations and the AFR image validates the analysis

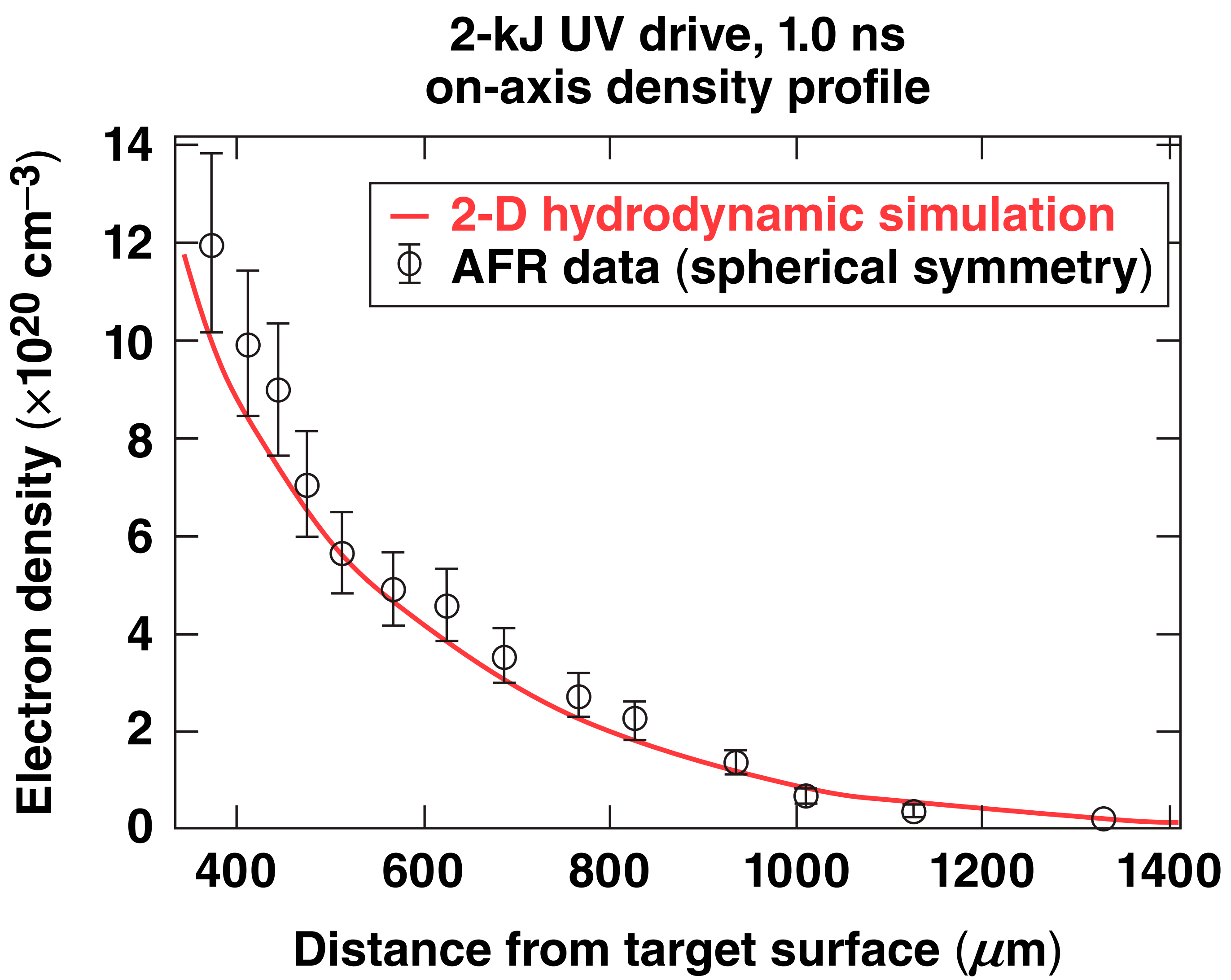

The plasma scale length is measured to be 250 μm by AFR.

E23461a

A single 10-ps, 1.2-kJ pulse channels up to ~0.6 n_c through the underdense corona

Channeling beam: 10 ps, 1.2 kJ, 125 TW, $I \cong 4 \times 10^{19}$ W/cm^2

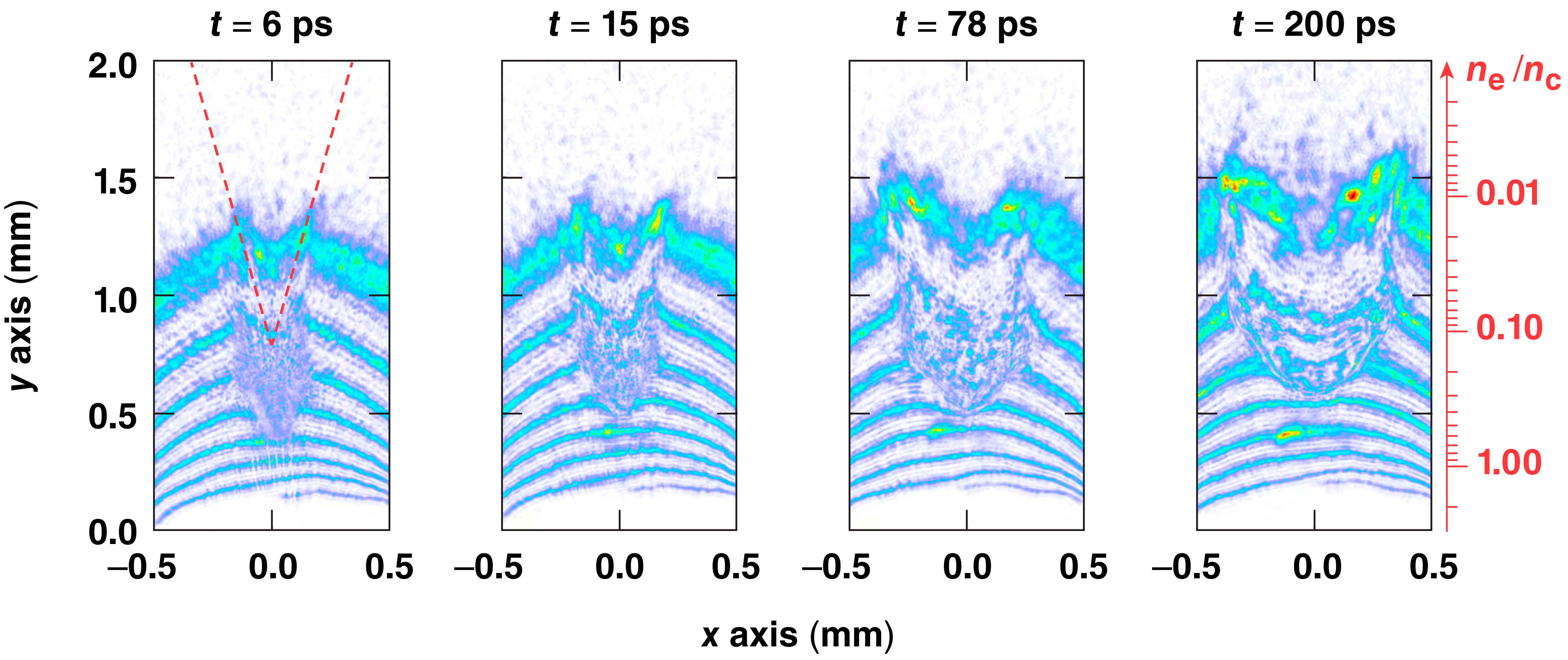

E23526a

S. Ivancic *et al*., Phys. Rev. E 9, 051101(R) (2015).

A single 100-ps, 2-kJ pulse bores to overcritical densities in the corona

Channeling beam: 100 ps, 2 kJ, 20 TW, $I \cong 4 \times 10^{18}$ W/cm^2

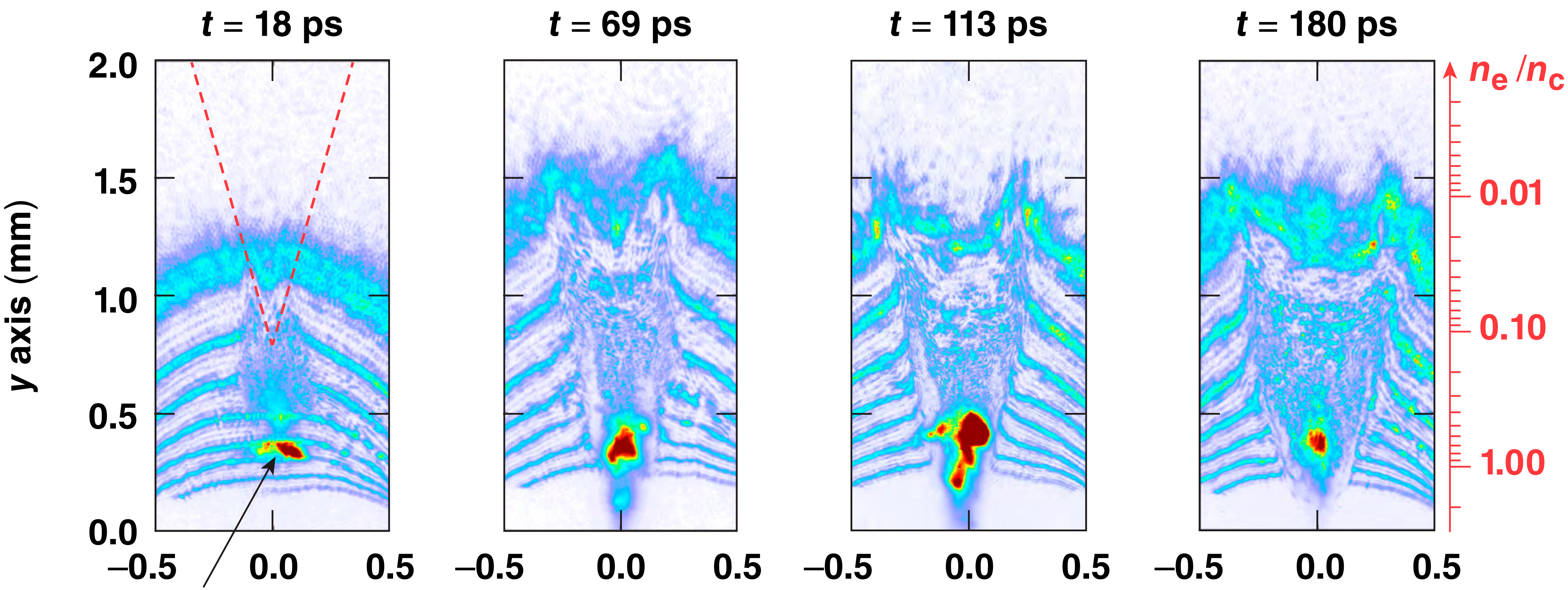

Fourth-harmonic self-emmision from a high-intensity laser

S. Ivancic *et al.*, Phys. Rev. E 9, 051101(R) (2015).

E23527a

The front of the channel moves forward from light pressure of the short-pulse beam

Reflection front

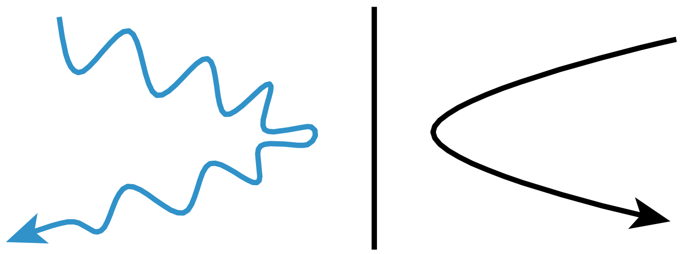

$$P^{+} = \frac{\rho v^{+2}}{2}$$

$$P^{-} = \frac{\rho v^{-2}}{2}$$

Light pressure at reflective interface

$$P_{L} = \frac{I}{c}(1 + R)$$

Forward-going plasma flow

$$P_{s} = \rho v_{ch}^{2}$$

- Assumptions
  - light is 100% reflected, $R = 1$
  - incoming and outgoing plasma flow are equal

- Equate pressures at the interface

$$\rho v_{c}^{2} = \frac{I}{c}(1 + R) \qquad \rho = n_{i} M = \frac{n_{e}}{Z} M \qquad v_{ch} = \sqrt{\frac{IZ(1+R)}{n_{e} M c}}$$

For an experiment on OMEGA EP: $n_{e} = 1.1 \times 10^{21}$, $Z = 3.5$, $I = 5.0 \times 10^{17}$ W/cm^{2}

$v_{ch} = 2.4\ \mu$m/ps $= 2400$ km/s

*W. L. Kruer, E. J. Valeo, and K. G. Estabrook, Phys. Rev. Lett. 35, 1076 (1975).

E24222

The extent of the channel head as a function of time follows a ponderomotive hole boring model*

Channel forward velocity balances with ablation velocity

$$v_{ch}(t) = \sqrt{\frac{I_L(t)Z(1+R)}{2n_e(y)m_i c}} - v_b$$

$$n_e(y) = n_0 e^{\frac{y}{L_s}}$$

$$I_L(t) = I_0 e^{-\left(\frac{t-50}{t_w}\right)^6}$$

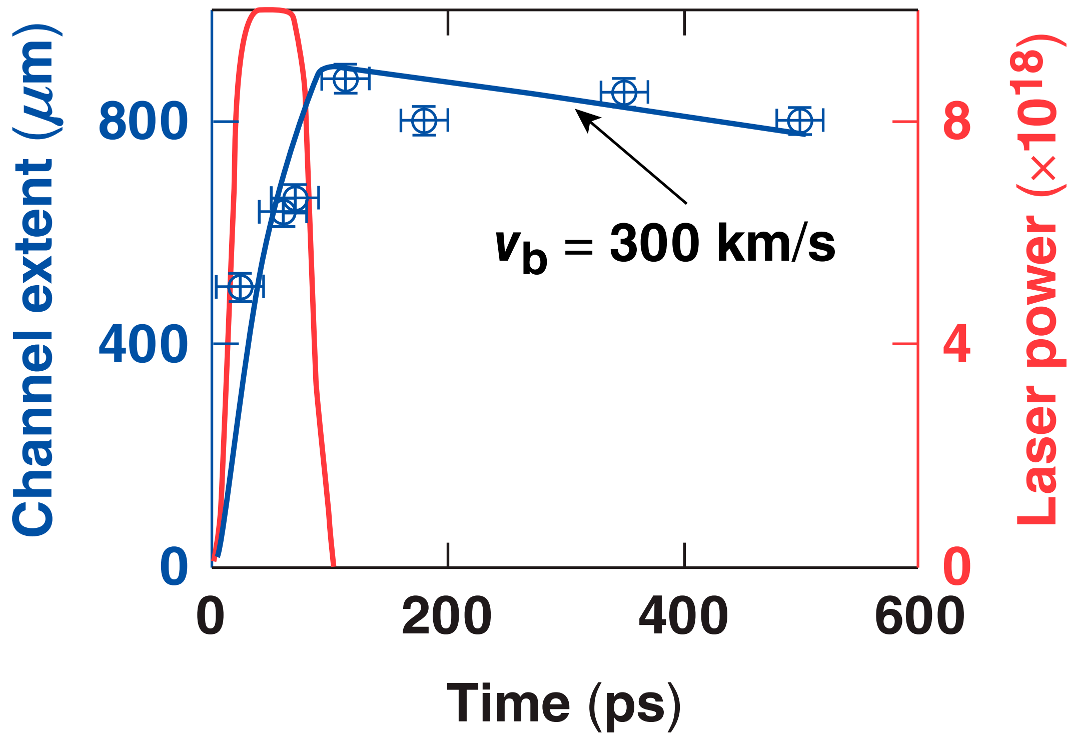

E24223

*S. C. Wilks *et al.*, Phys. Rev. Lett. 69, 1383 (1992).

The residual density in the channel is found through an Abel inversion of the AFR image

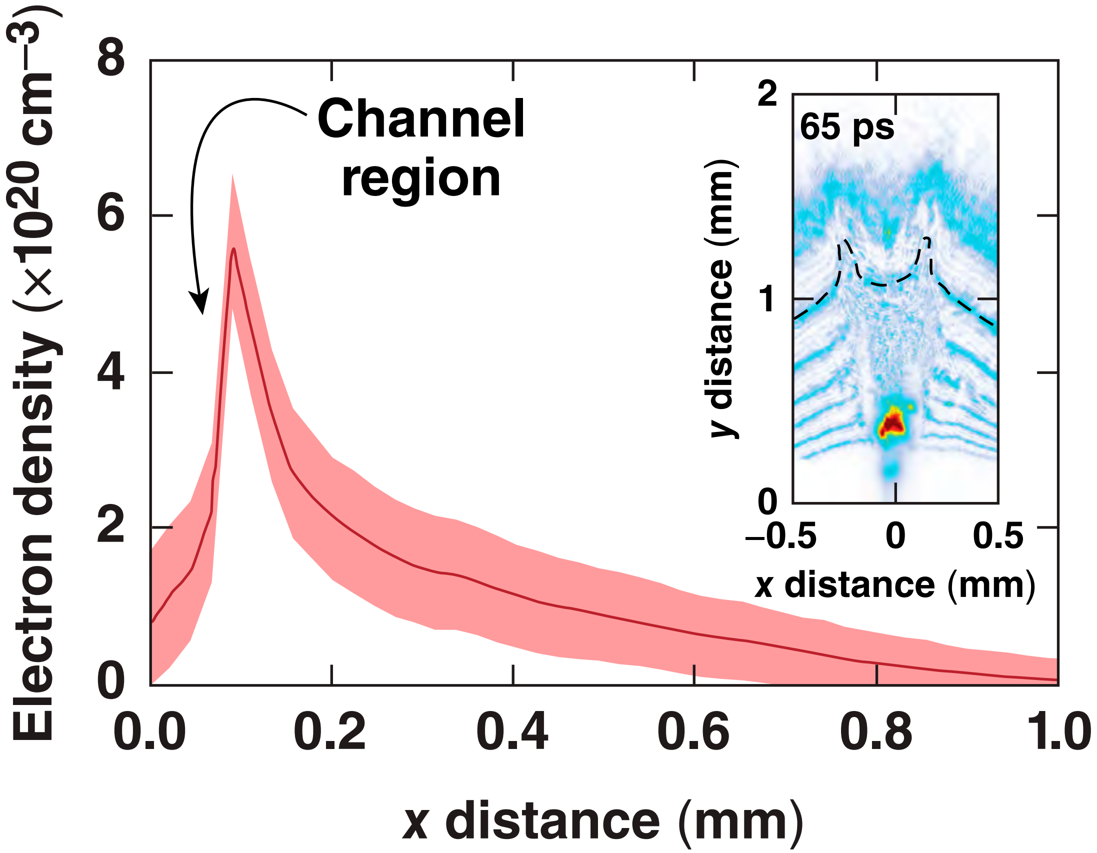

$$n_e(r) = \frac{-2n_c}{\pi}\int_r^{\infty}\theta_x(x)\frac{dx}{\sqrt{x^2-r^2}}$$

The density in the channel is reduced to $(1\pm0.75)\times10^{20}$ cm^{-3}

S. Ivancic *et al.*, Phys. Rev. E 9, 051101(R) (2015).

E23463

Shadowgraphs of the channel expansion as a function of time were obtained

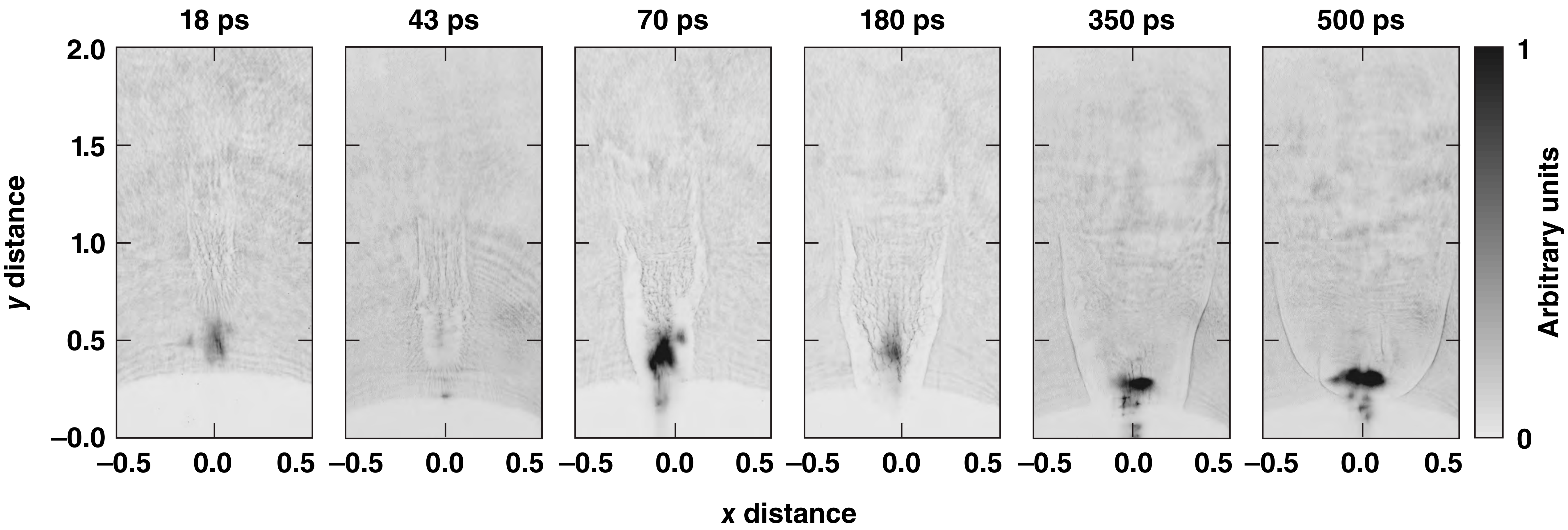

The channel radius evolves in a self-similar manner.

A self-similar cylindrical model is used to explain the expansion of the channel as a function of time

- Expansion is modeled by Sedov in a cylindrical blast wave*

  R(t) = channel radius
  E_{th} = thermal deposition per unit length
  ρ_0 = density at laser focus
  t_0 = timing offset

	E_{th} (J/mm)
100 ps	150±61
10 ps	234±150

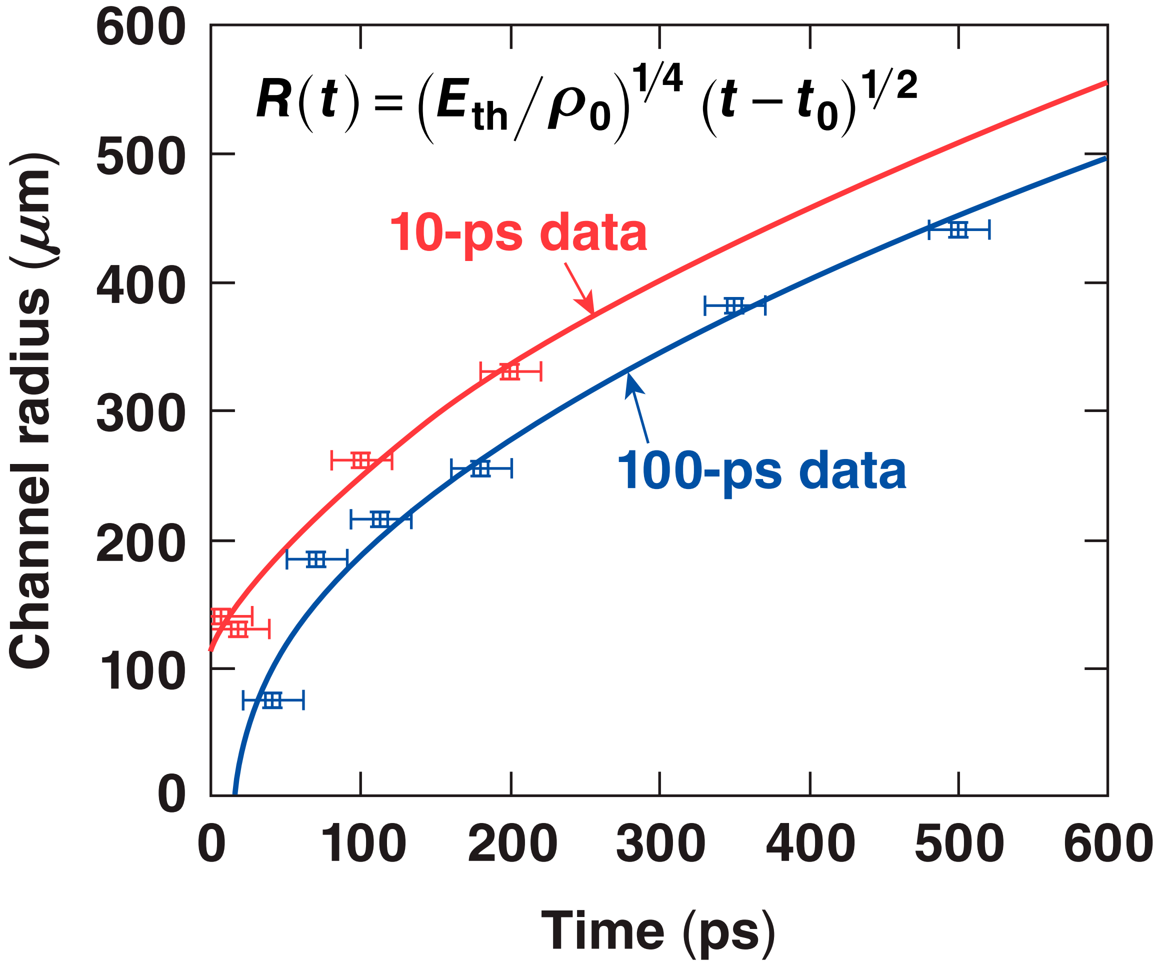

E24225

*L. I. Sedov, Prikl. Mat. Mekh. 10, 241 (1946).

Radiation–hydrodynamics simulations show the channel cooling is consistent with expansion

UR LLE

- **Uniformly heated volume was incorporated into the simulation**
- **There was excellent agreement between the self-similar expansion model and radiation–hydrodynamics model**

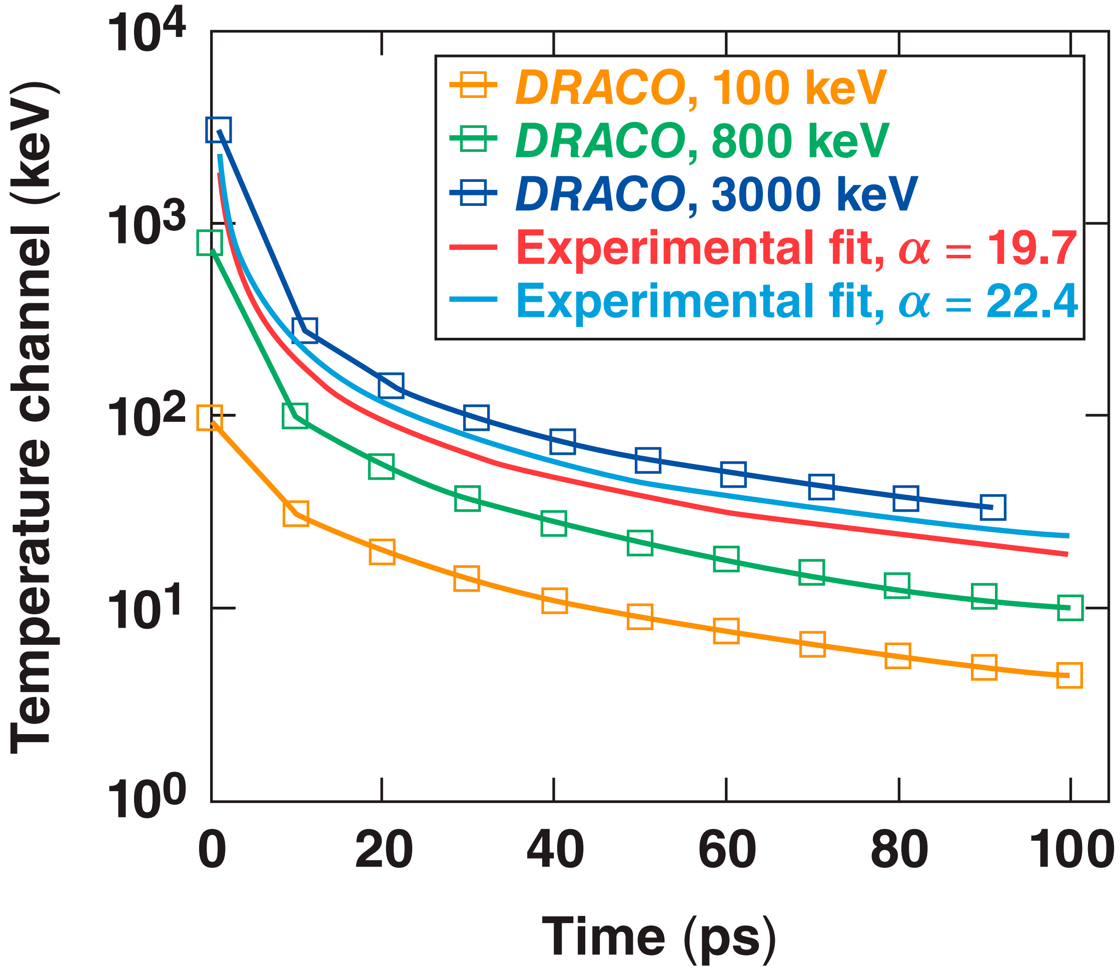

E24226

Experiments with co-propagating 100-ps and 10-ps pulses were performed

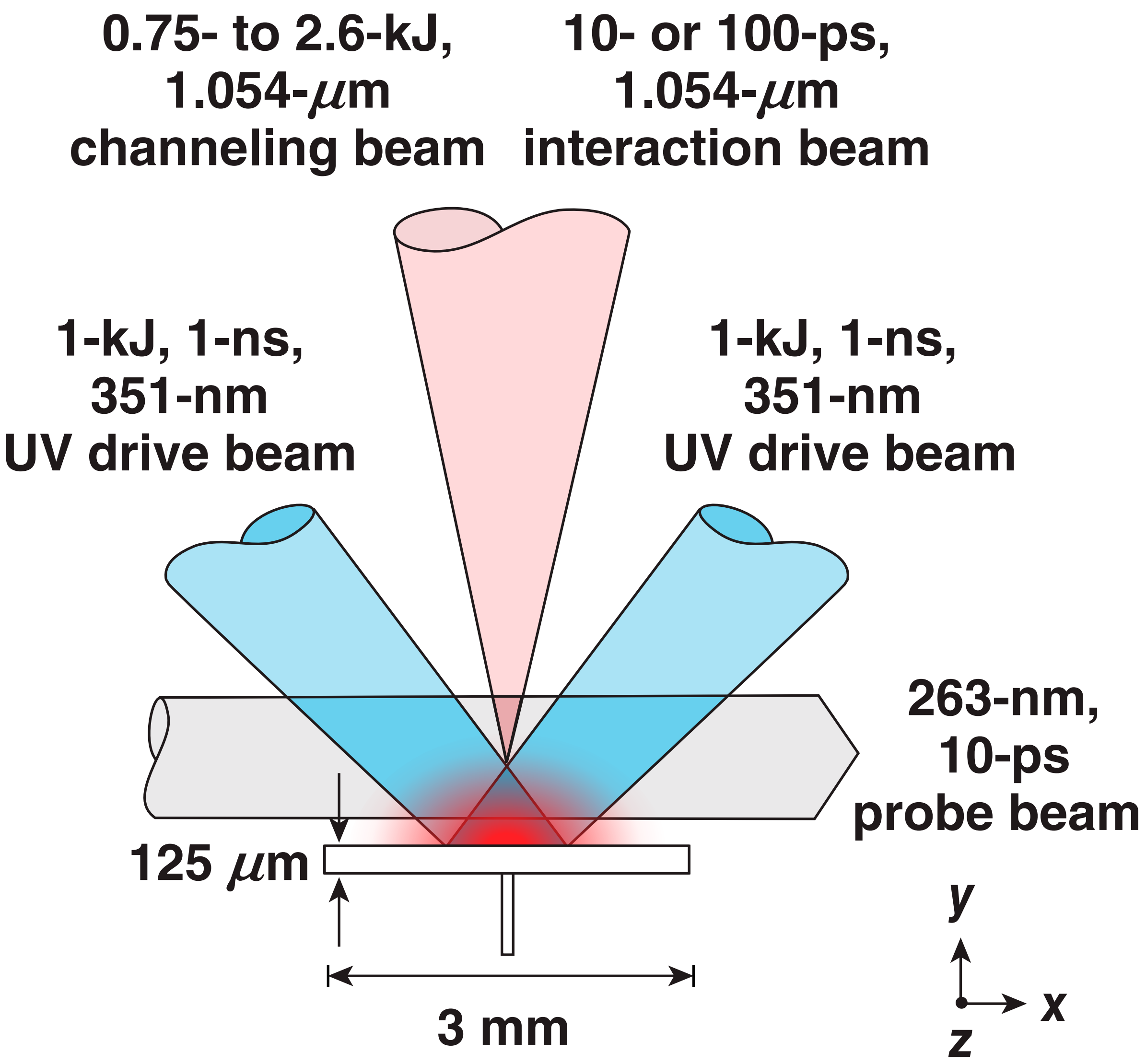

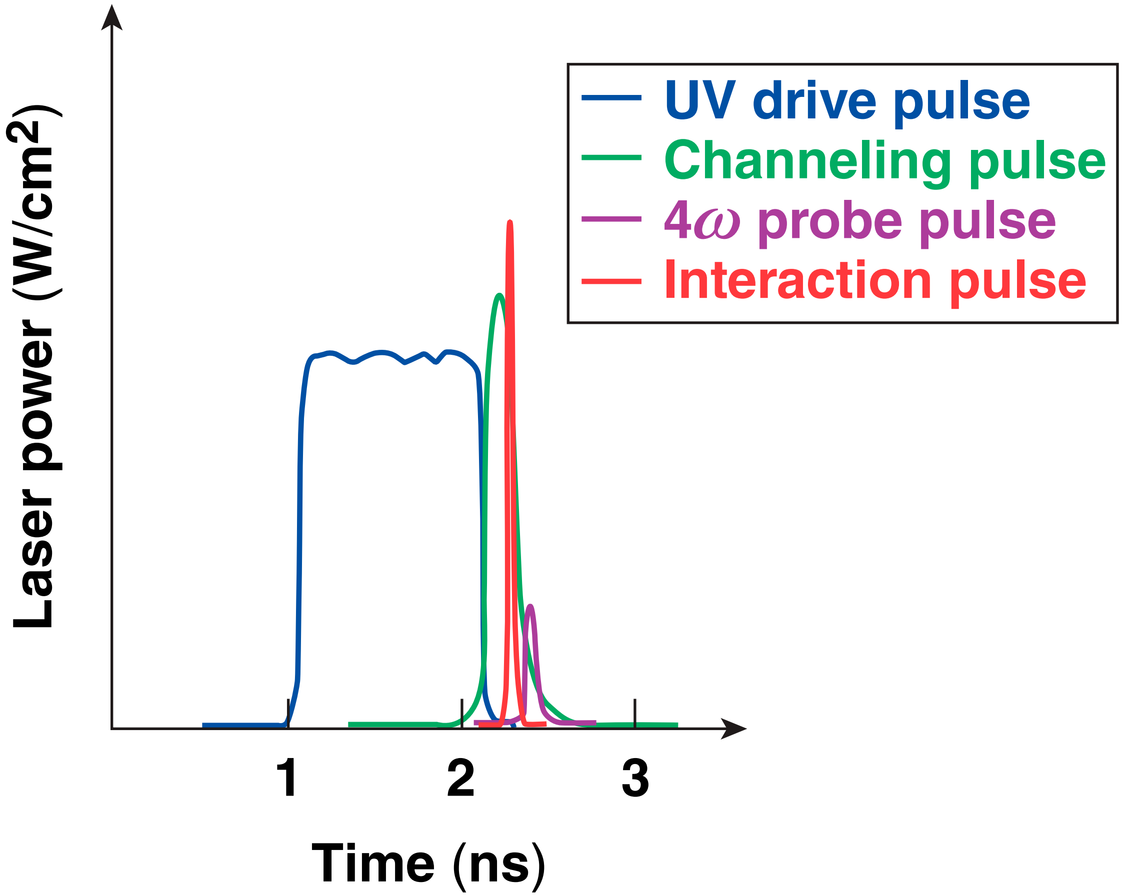

E24227

The channel allows for the efficient transport of a second laser pulse

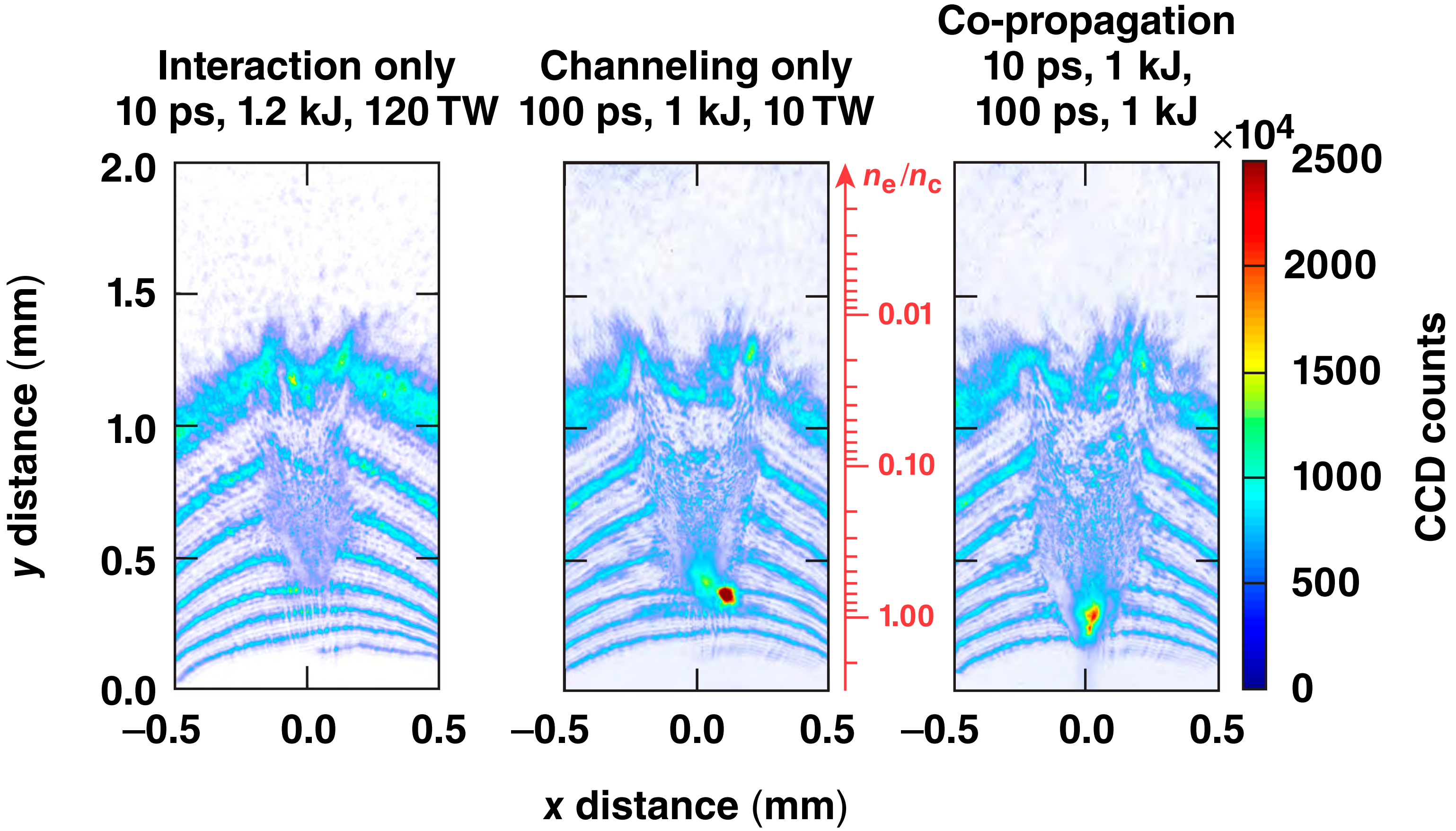

E24228

The channel allows for the efficient transport of a second laser pulse

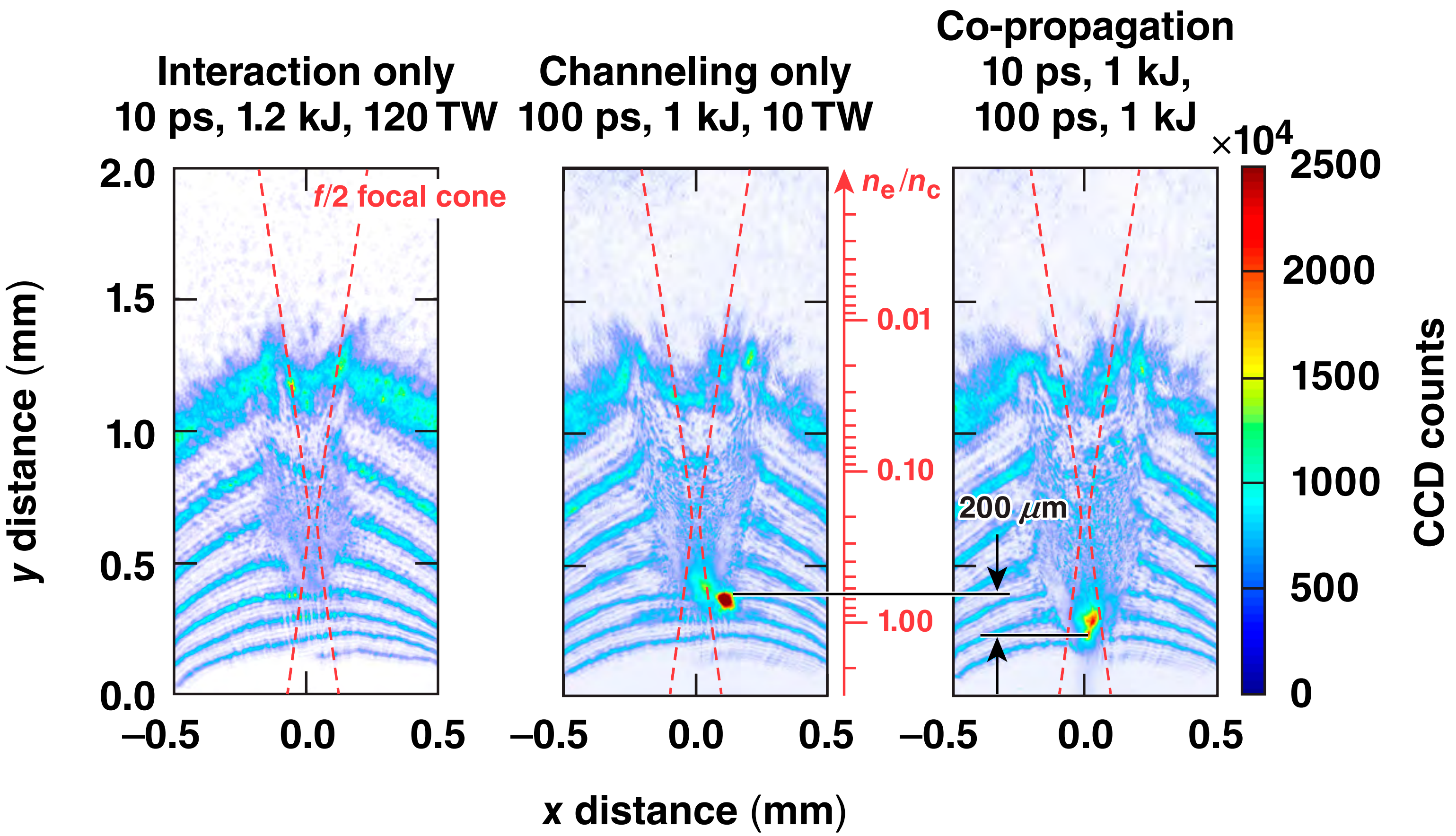

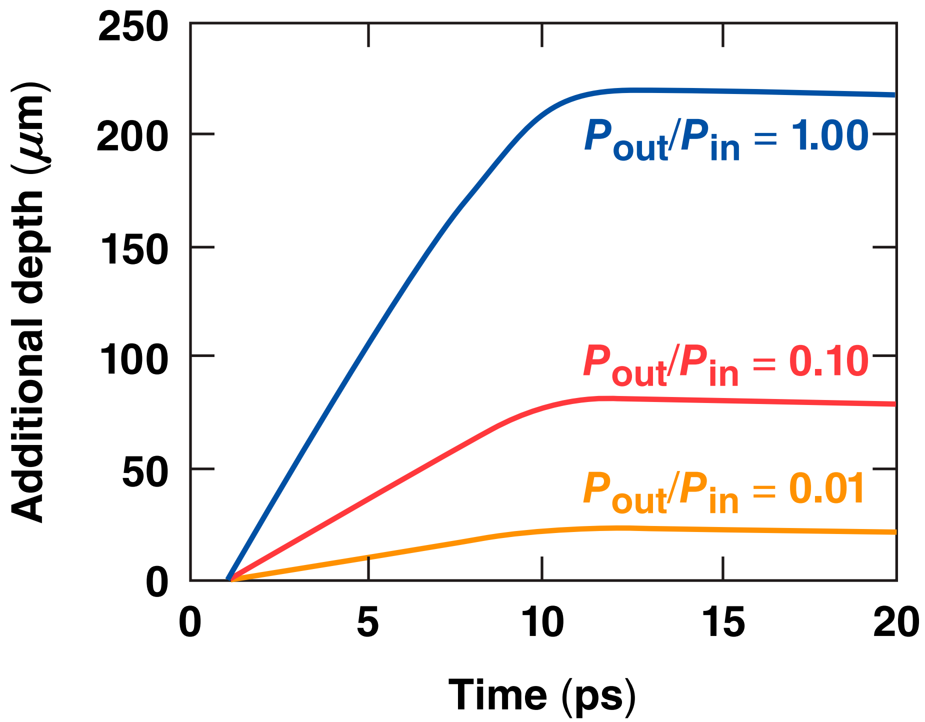

E24228a

Summary/Conclusions

OMEGA EP experiments show for the first time the guiding of a high-intensity pulse to beyond critical density in a fast-ignition (FI)–relevant, long-scale-length plasma

- Angular filter refractometry (AFR)* is used to observe the density modification of a channel beyond critical IR density (1.4×10^{21} cm^{-3})
- A high-intensity (>10^{18} W/cm^2) laser evacuates a conical-shaped cavity with ~65% lower density than the background density
- A 100-ps, 1-kJ laser pulse produced a channel beyond critical, allowing for the efficient transmission of a high-intensity ($I \cong 4 \times 10^{19}$ W/cm^2) co-propagated pulse to beyond critical density

*D. Haberberger *et al*., Phys. Plasmas 21, 056304 (2014).

E23522a

The OMEGA EP fourth-harmonic (4ω) probe laser system* delivers a probe beam to the target chamber that is collected at *f*/4

Target chamber center illumination

- *f*/25 diverging illumination beam
- 3.3-mm-diam beam presented to experimental region
- All spherical *f*/4 catadioptric meniscus telescope

Diagnostic table

- 3.6-μm resolution
- 3.7 × 3.7-mm field of view
- Three 2k × 2k scientific cameras

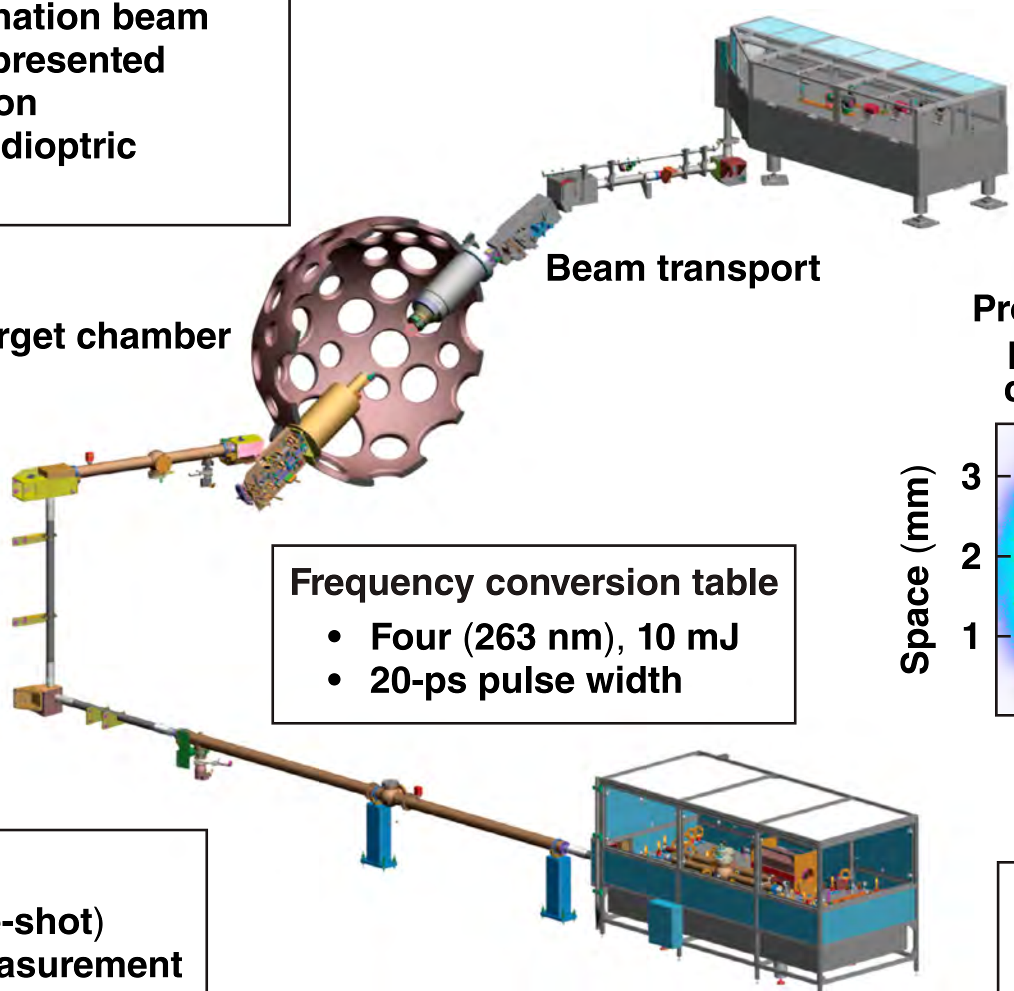

Frequency conversion table

- Four (263 nm), 10 mJ
- 20-ps pulse width

Timing

- ±50-ps accuracy (pre-shot)
- ±20-ps post-shot measurement

Probe beam spatial profile at target chamber center

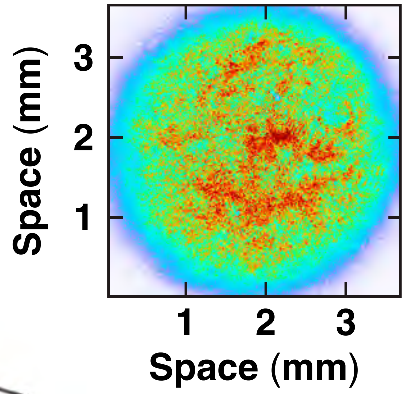

Probe alignment grid

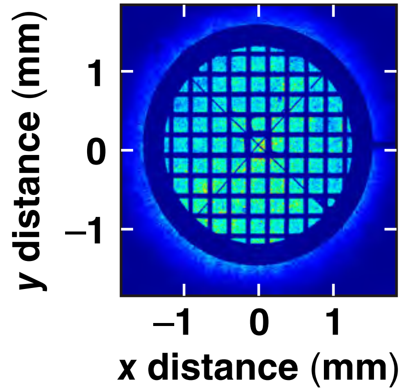

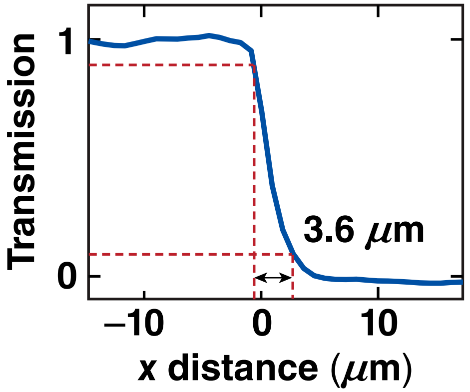

Nd:glass laser

- 1053-nm, 100-mJ pulse
- ~20-ps pulse width

E22054e

*D. H. Froula *et al*., Rev. Sci. Instrum. 83, 10E523 (2012).

A spherical plasma model can be used to estimate the divergence caused by propagation through plasma

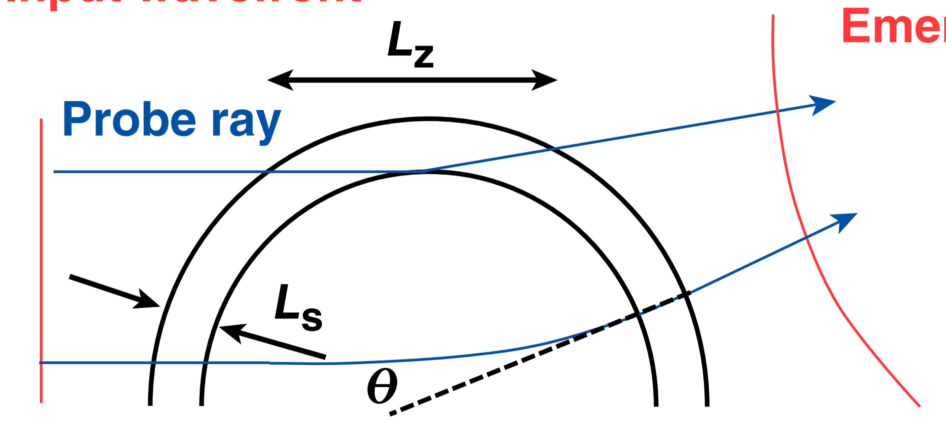

Phase shift through plasma $\Phi = \frac{\omega}{c}\int_0^{L_z} N dl = \frac{\omega}{c}\int_0^{L_z}\sqrt{1-\frac{n_e}{n_c}}\,dl \approx \frac{\omega}{2cn_c}\int_0^{L_z} n_e dl$

$$\Phi = \frac{\lambda}{\pi n_c}\int_0^{L_z} n_e dl, \quad n_c = \frac{1.1\times 10^{21}\ \text{cm}^{-3}}{\lambda^2_{\mu m}}$$

Ray divergence through plasma $\theta = \frac{2\pi}{\lambda}\frac{\partial\Phi}{\partial r} \cong \frac{n_e L_z}{n_c L_s}$

Assumptions:

$n_e < n_{c,\text{probe}}$

$\theta \ll 1\,(\text{radian})$

$L_z = L_s\sqrt{1+\frac{2r}{L_s}}$

The refracted angle of the ray is related to the plasma density and a geometric factor defined by the ratio of scale length to the transverse dimension.

The AFR transform can be thought of as a filtering process in the spatial frequency domain

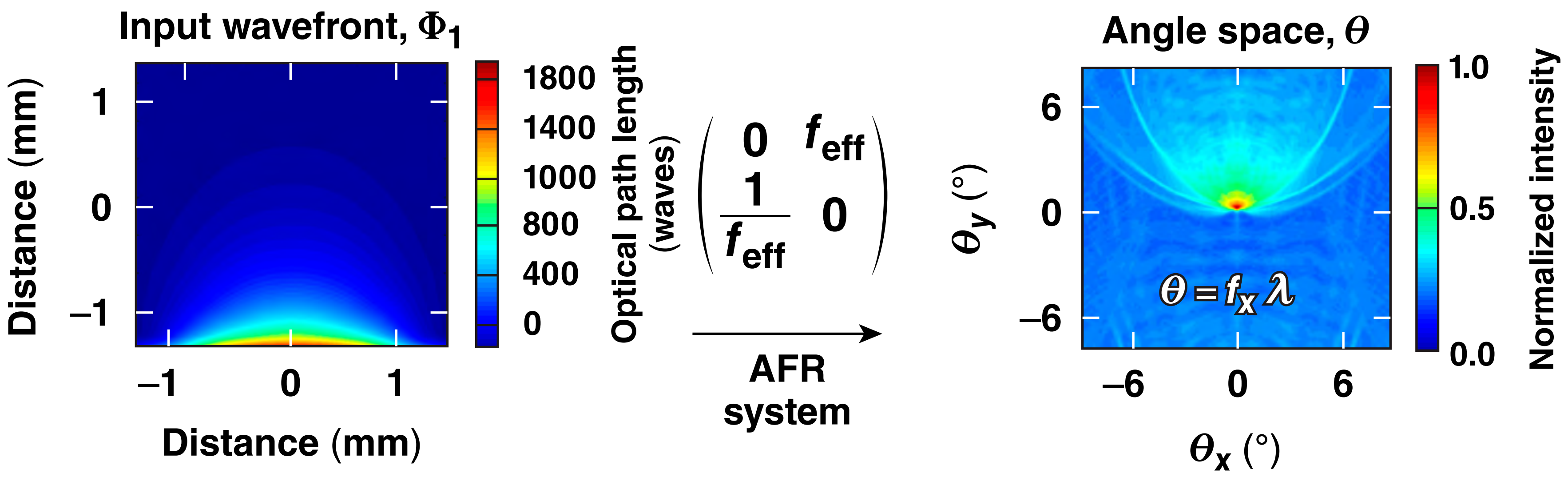

- Integral transform between plane P_1 and P_2

$$I_2(f_x,f_y)=\iint \Phi_1(x,y)\exp\left\{\frac{i\pi}{\lambda a_{12}}\left[a_{11}(x^2+y^2)-2(xf_x+yf_y)+a_{22}(f_x^2+f_y^2)\right]\right\}dxdy$$

$$I_2(f_x,f_y)=\iint \Phi_1(x,y)\exp\left\{\frac{i\pi}{\lambda f_{eff}}\left[-2(xf_x+yf_y)\right]\right\}dxdy$$

a_{11} and a_{22} = 0 is required

E22845a

The AFR transform can be thought of as a filtering process in the spatial frequency domain

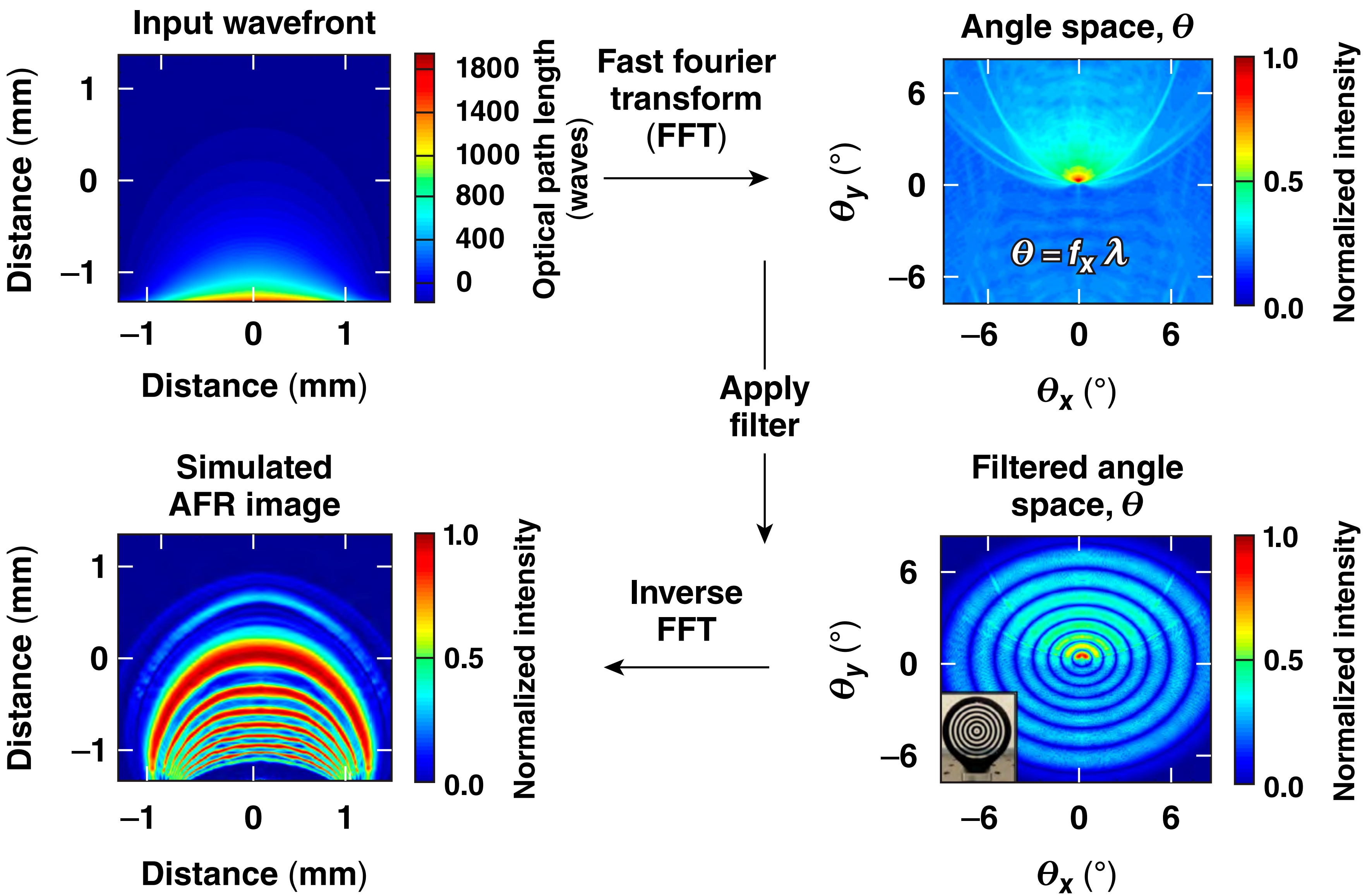

E22845b

AFR of a UV ablation plasma

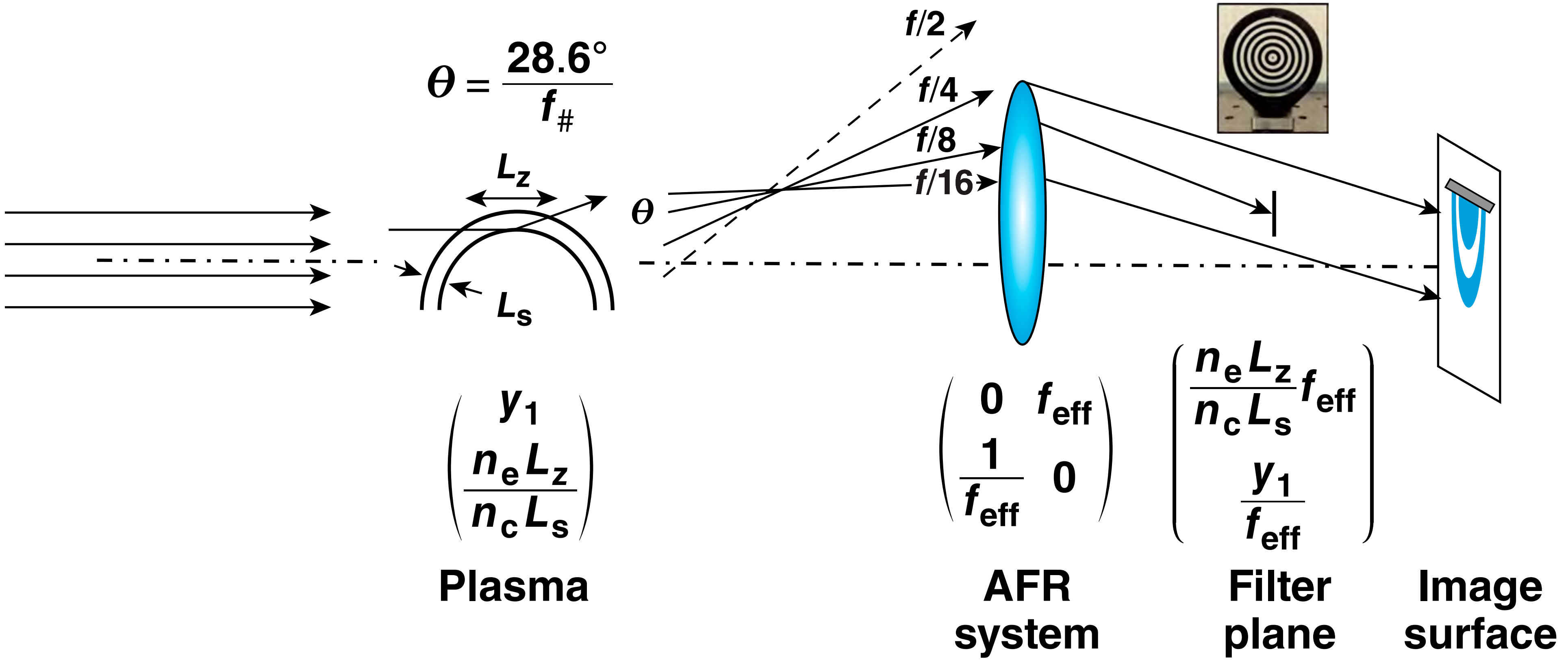

- Using the angle as before, we find that the rays' height in the filtering plane are a function of plasma density; installing a block of varying radii, we can discriminate the density the rays were refracted from

The signal is filtered at the image plane by the angle it enters the AFR system. The position of the signal on the image plane is unchanged by the AFR system.

E24219

The observed channel progression is consistent with particle-in-cell (PIC) simulations*

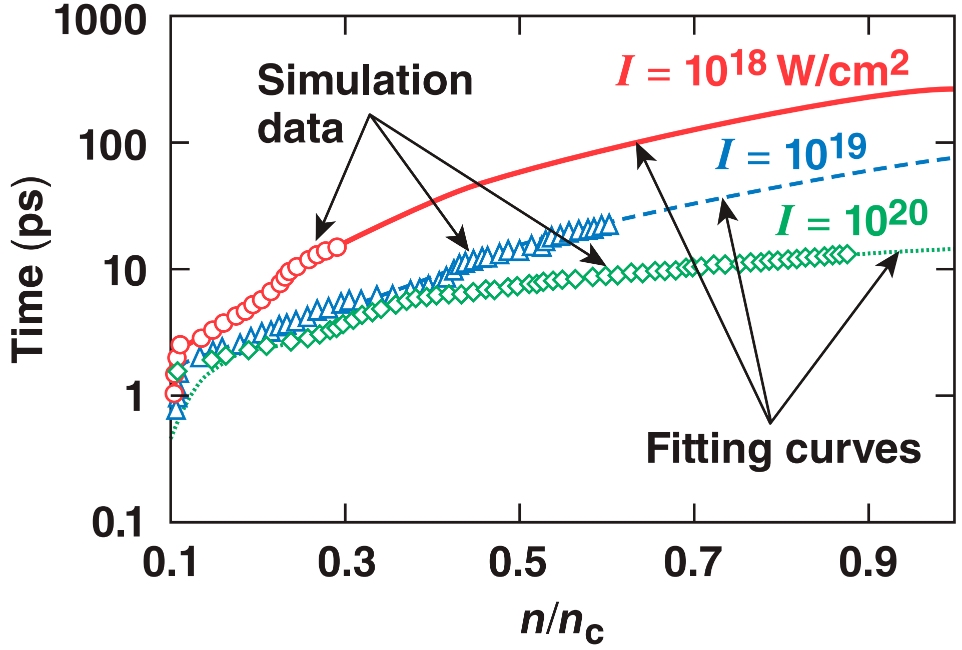

- Scaling laws for the required time and energy for channel to reach n_c**

$$T(\text{ps}) = 150\ I_{18}^{-0.64},\ E(\text{kJ}) = 0.85\ I_{18}^{-0.32}$$

$$2 \times 10^{18}\ \text{W/cm}^2\text{: }100\ \text{ps},\ 1\ \text{kJ};\ 2 \times 10^{19}\ \text{W/cm}^2\text{: }15\ \text{ps},\ 2.2\ \text{kJ}$$

The 100-ps pulse has sufficient energy to reach the critical density, while the 10-ps pulse lacks energy to reach the critical density.

*G. Li *et al.*, Phys. Rev. Lett. 100, 125002 (2008).
**G. Li *et al.*, Phys. Plasmas 18, 042703 (2011).